

**Supplementary Information**

**In Situ Anion-Driven Reconstruction of NiS for High-Performance**

**Benzyl Alcohol Electrooxidation**

Wenshu Yang, Yitian Wu, Zhenghao Zhang, Qianwen Qiu, Xiao Yang, Longhua Li,

Jinhui Hao\* Weidong Shi\*

School of Chemistry and Chemical Engineering, Jiangsu University, Zhenjiang

212013, China

*Email: jinhui\_hao@ujs.edu.cn; swd1978@ujs.edu.cn*

## **EXPERIMENTAL SECTION**

### **Materials**

Benzyl alcohol (BA) (99.9 wt.%), Benzoic acid (BAC), benzaldehyde (99.9 wt.%), potassium hydroxide, sodium hypophosphite, sulfur powder, methanol (HPLC-grade), ethanol, and NF were purchased from Sinopharm Chemical Reagent Co.

### **Preparation of Catalysts**

The catalysts were prepared by the combination of electrodeposition and calcination methods. The NF was cleaned with 1M HCl for 10 minutes to remove the surface NiO layer, and then ultrasonicated in ethanol and deionized water for 5 minutes, respectively. Then, the clean NF was placed in a two-compartment H-type electrolytic cell containing 0.1M Ni(NO<sub>3</sub>)<sub>2</sub> solution with a saturated Ag/AgCl as the reference electrode. The electrodeposition process was carried out under chronopotentiometry (CP) technique for 10 minutes. Following electrodeposition, the samples were rinsed with deionized water and subsequently dried in an oven at 60 °C. NiO/NF was synthesized by directly calcining the sample in a tube furnace. After purging with argon for about 30 minutes, the sample was heated to 350 °C and maintained for 2 hours. For the synthesis of Ni<sub>2</sub>P/NF, sodium hypophosphite (NaH<sub>2</sub>PO<sub>2</sub>·H<sub>2</sub>O, 100 mg) was placed in a separate porcelain boat at the upstream end, while the dried sample was positioned in a porcelain boat at the downstream end of the tube furnace. After purging with argon for about 30 minutes, the sample was heated to 400 °C and maintained for 1.5 hours. The synthesis method of NiS/NF is similar to that of Ni<sub>2</sub>P/NF. The dried sample was placed at the downstream of the tube furnace, and sulfur powder (S, 150 mg) was placed in the porcelain boat at the upstream. After purging with argon for about 30 minutes, the sample was heated to 350 °C and maintained for 0.5 hours.

### **Materials characterization**

X-ray diffraction (XRD) was carried out using a smartlab9 X-ray diffractometer

(Rigaku, Japan) to characterize the crystal structure of the catalysts. Scanning electron microscopy (SEM) was carried out with a Hitachi S-4800 to characterize the surface morphology of the catalysts. X-ray photoelectron spectroscopy (XPS) was carried out using a Thermo Fisher Scientific Escalab 250Xi instrument. The instrument used for the electron spin resonance (EPR) was manufactured by BRUKER (Germany), model A300-10/12.

### **Electrochemical measurements**

Electrochemical measurements were carried out using the CHI660E electrochemical workstation. A three-electrode system was constructed using an H-type electrolytic cell. The synthesized samples, carbon glass, and the Hg/HgO were used as working electrode, counter electrode, and reference electrode, respectively. The electrolytic solution was either 1 M KOH or 1 M KOH + 0.1 M BA. All test voltages were converted to RHE using the following equation:  $E(RHE) = E(Hg/HgO) + 0.059 \times pH + 0.098V$ . Linear scanning voltammetric curves were performed at a sweep rate of  $5 \text{ mV s}^{-1}$ . (No iR infrared correction was performed during the test.) The electrochemical double layer capacitance ( $C_{dl}$ ) was calculated from cyclic voltammetry (CV) data. Electrochemical impedance (EIS) measurements were carried out at 0.6 V (vs. Hg/HgO) with applied frequency from  $10^{-2}$  to  $10^5$  Hz. The amperometric i-t curve (i-t) was performed at 1.52 V vs. RHE. The CP method was performed at  $10 \text{ mA cm}^{-2}$  for electrodeposition.

### **Product analysis**

The products for BA oxidation were detected by a high-performance liquid chromatography (HPLC) system using a C18 column ( $4.6 \times 250 \text{ mm}$ ) and an ultraviolet-visible detector (UV) for qualitative and quantitative analysis. For electrolysis, 200  $\mu\text{L}$  of electrolyte was taken and diluted to 10 mL with ultrapure water,

and then analyzed by HPLC. The mobile phase was a mixture of methanol and water (4:6) at a flow rate of 0.6 mL min<sup>-1</sup>. The conversion of BA can be calculated from the following equation (1):

$$\text{Conversion} = \frac{n_{\text{reacted} - \text{BA}}}{n_{\text{initial} - \text{BA}}} \times 100\% \quad (1)$$

The conversion and yield of BAC were determined as in the following equations (2) and (3) :

$$\text{Selectivity} = \frac{n_{\text{BAC} - \text{production}}}{n_{\text{reacted} - \text{BA}}} \times 100\% \quad (2)$$

$$\text{Yield} = \frac{n_{\text{BAC} - \text{production}}}{n_{\text{initial} - \text{BA}}} \times 100\% \quad (3)$$

The efficiency of the product is calculated using Faraday's formula:<sup>1</sup>

$$FE = \frac{4 \times n \times 96485}{Q_{\text{total}}} \times 100\% \quad (4)$$

where  $Q_{\text{total}}$  is the total charge consumed during BOR and  $n$  is the moles of BAC.

### DFT calculations

Density functional theory (DFT) calculations were performed on a periodic slab model (2×2 surface supercell, 4 atomic layers, with the bottom 2 layers fixed and with a vacuum layer thickness of approximately 15 Å).<sup>2</sup> A plane-wave basis set with a 450 eV projected augmented wave (PAW) exchange correlation function using the PBE generalized gradient approximation was employed. A 3×3×1 Monkhorst-Pack grid was used to sample k-points in the Brillouin zone.<sup>3</sup> Geometric optimization was considered converged when residual forces fell below 0.02 eV/Å and energy convergence was achieved at 1×10<sup>-5</sup> eV. The Fermi energy level was set to zero as the energy reference frame.<sup>4</sup>



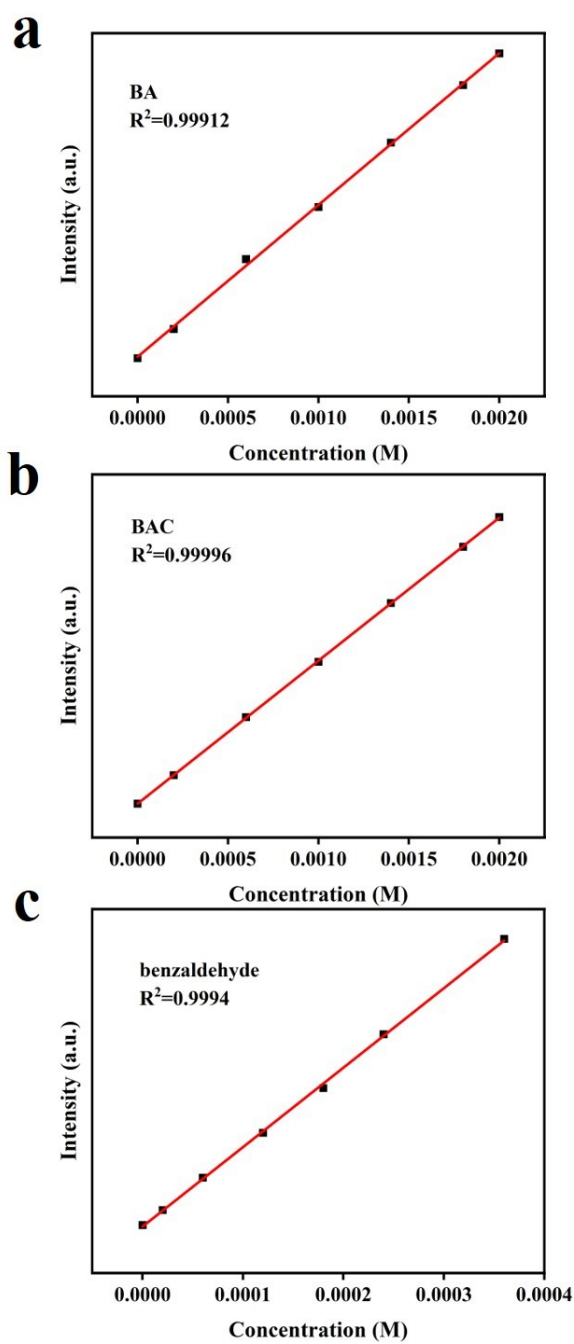


**Figure S1** The standard curves of liquid chromatography for BA (a), BAC (b) and benzaldehyde product (c).

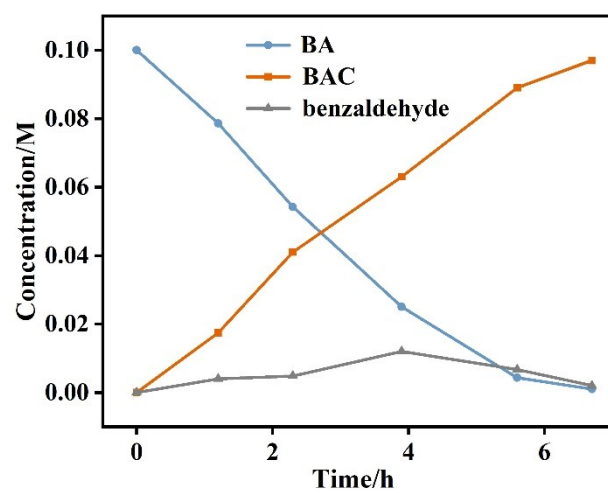


**Figure S2** The concentrations of reactants and products at different reaction times.

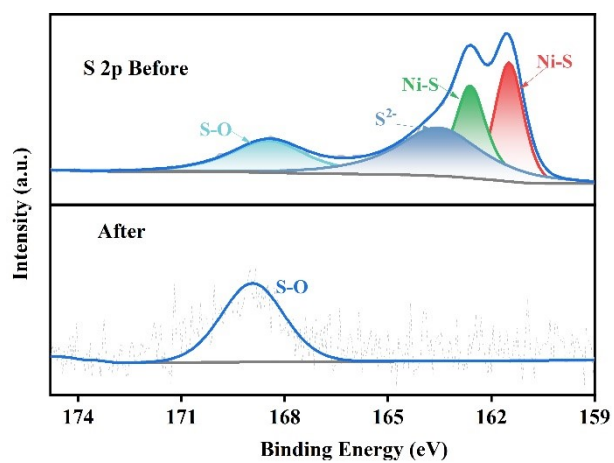


**Figure S3** S 2p XPS spectra of NiS/NF before and after reaction.

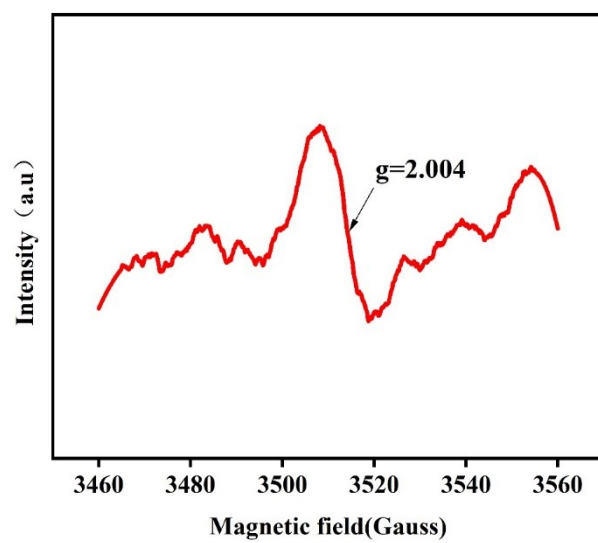


**Figure S4** EPR spectrum of NiS/NF.

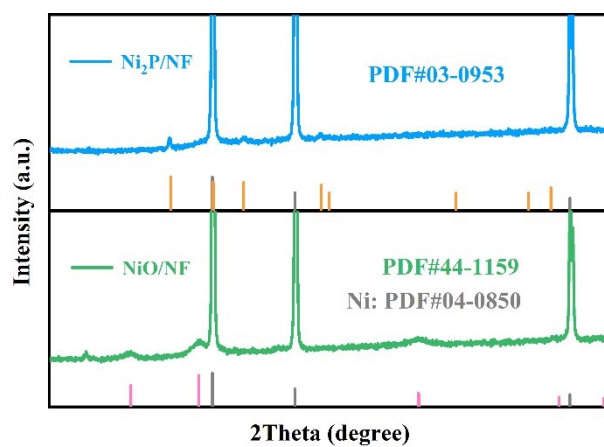


**Figure S5** XRD patterns of  $\text{Ni}_2\text{P}/\text{NF}$  and  $\text{NiO}/\text{NF}$

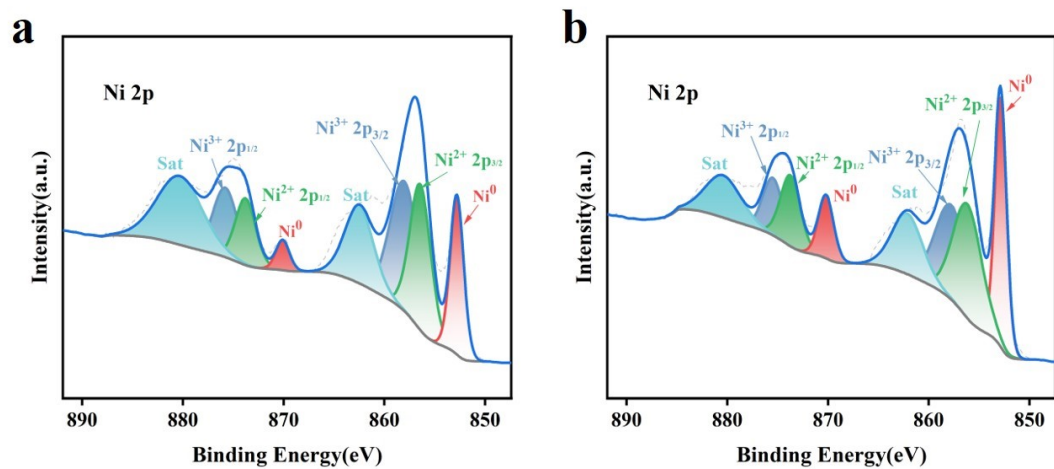


**Figure S6** Ni 2p XPS spectra of Ni<sub>2</sub>P/NF (a) and NiO/NF (b)

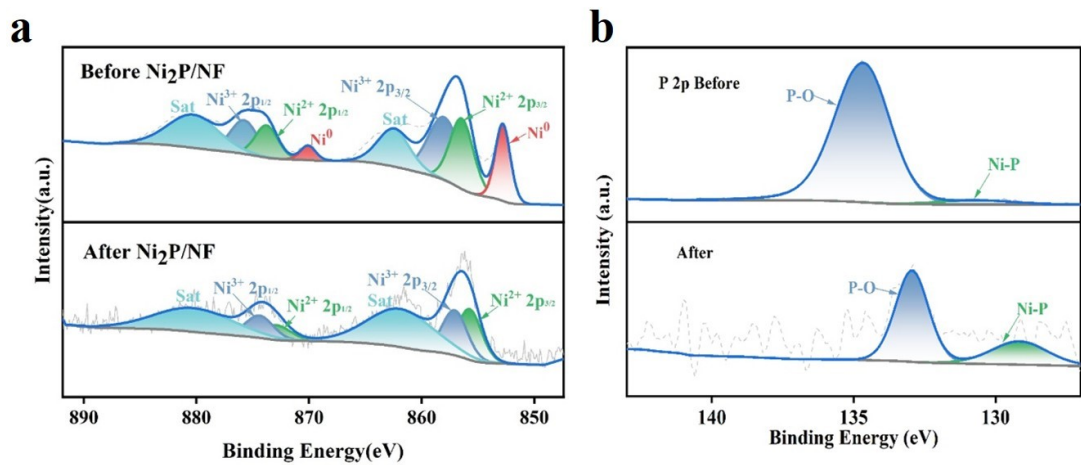


**Figure S7** XPS spectra of Ni 2p (a) and P 2p(b) for Ni<sub>2</sub>P/NF before and after reaction

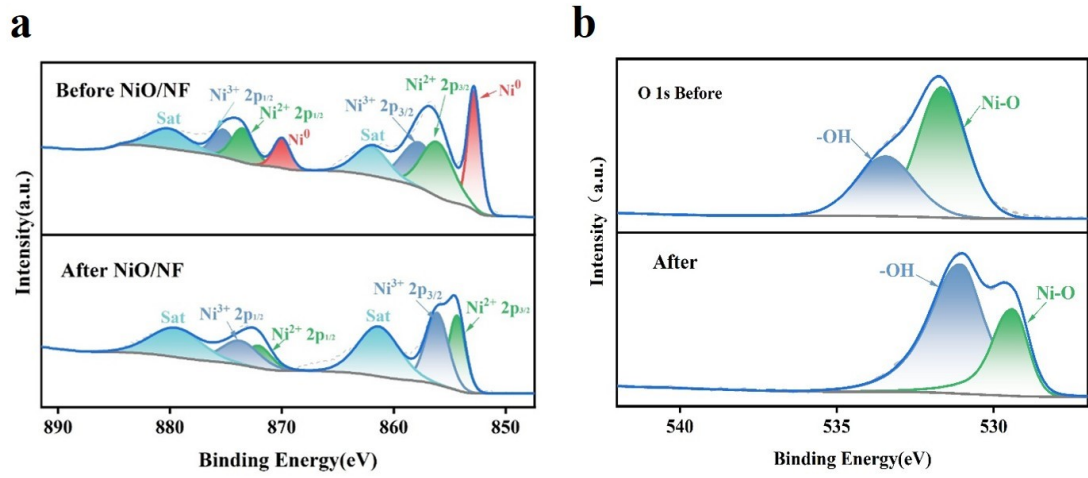


**Figure S8** XPS spectra of Ni 2p (a) and O 1s (b) for NiO/NF before and after reaction

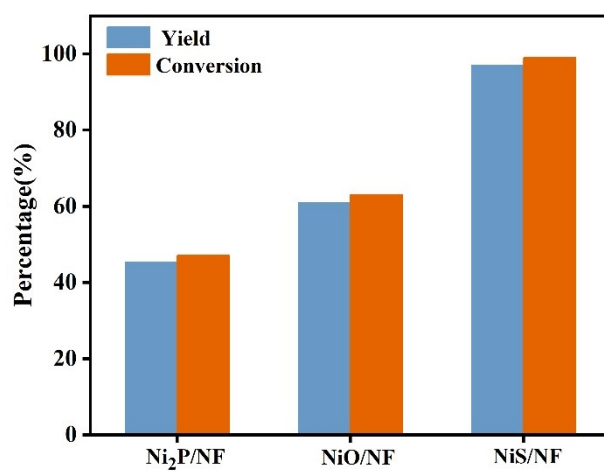


**Figure S9** Conversion rates and yields of three catalysts under identical conditions

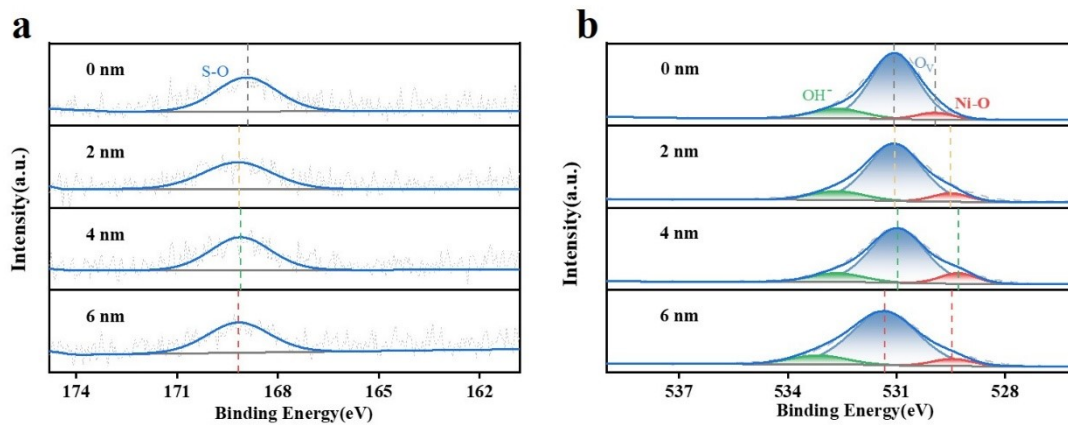


**Figure S10** (a) S 2p XPS depth profiling by argon ion sputtering of NiS/NF. (b) O 1s XPS depth profiling by argon ion sputtering of NiS/NF.



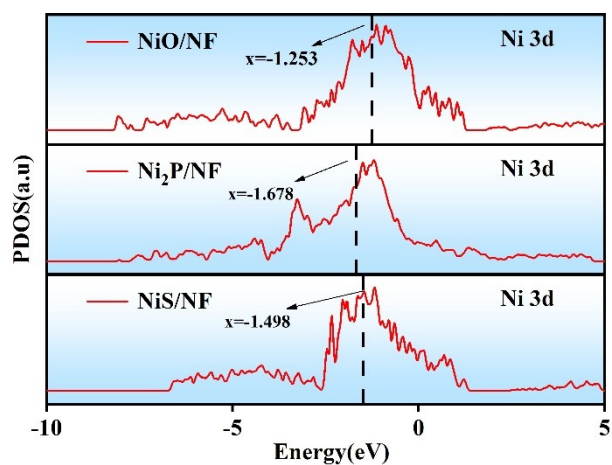


**Figure S12** PDOS of Ni d-band in three catalysts.

**Table S1** Fitted EIS parameters of NiS/NF, Ni<sub>2</sub>P/NF and NiO/NF

Catalysts	R <sub>s</sub> ( $\Omega$ )	R <sub>int</sub> ( $\Omega$ )	CPE <sub>1</sub> -T ( $10^{-5}$ $F^{-1}\cdot s^{1-n}$ )	CPE <sub>1</sub> -P	R <sub>ct</sub> ( $\Omega$ )	CPE <sub>2</sub> -T $F^{-1}\cdot s^{1-n}$	CPE <sub>2</sub> - P
NiS/NF	1.40	0.92	0.42	0.94	2.99	0.08	0.71
Ni <sub>2</sub> P/NF	1.41	0.83	0.91	0.88	4.10	0.05	0.72
NiO/NF	1.36	1.13	1.41	0.83	3.86	0.11	0.74

## References

- 1.H. Chen, Z. Zhu, Y. Zhu, M. Kuai, K. Chai and W. Xu, *New Journal of Chemistry*, 2024, **48**, 10925-10934.
- 2.G. Kresse and J. Hafner, *Physical Review B*, 1993, **48**, 13115-13118.
- 3.H. Park, Y. Kim, S. Choi and H. J. Kim, *Journal of Energy Chemistry*, 2024, **91**, 645-655.
- 4.C. He, P. Shi, D. Pang, Z. Zhang and L. Lin, *Molecular Catalysis*, 2022, **524**, 112327.